AIAA JOURNAL
Vol. 49, No. 12, December 2011

Energetically Optimal Short-Range Gliding Trajectories for Gliding Animals

David Willis*
University of Massachusetts Lowell, Lowell, Massachusetts 01854
and
Joseph Bahlman,† Kenneth Breuer,‡ and Sharon Swartz§
Brown University, Providence, Rhode Island 02912

DOI: 10.2514/1.J051070

Maximum range in steady-state glides is achieved when the lift coefficient is chosen to maximize the lift-to-drag ratio. Whether or not this same steady-state result applies to animal gliders is examined. Because animal gliders spend relatively little time in the air and glide relatively short distances, it is expected that the transient behavior at the beginning and end of the glide will govern their performance. A time-dependent, two-dimensional computational dynamics model is used to predict glide trajectories for biologically inspired gliders. The results demonstrate that glide range is greatest when the lift coefficient does not correspond to that predicted by classical steady-state gliding theory. This indicates that the transient dynamics of short-range gliders are important in maximizing their range.

Nomenclature

$a_t(t)$	=	acceleration component tangent to the flight path, m/s^2
$a_n(t)$	=	acceleration component normal to the flight path, m/s^2
$a_R(t)$	=	resultant acceleration, m/s^2
b	=	wing span, m
$C_D(t)$	=	glider drag coefficient ($C_D = \frac{D}{\frac{1}{2}\rho V_\infty^2 S}$)
C_{D_o}	=	zero-lift drag coefficient
$C_L(t)$	=	glider lift coefficient ($C_L = \frac{L}{\frac{1}{2}\rho V_\infty^2 S}$)
c	=	wing chord, m
$D(t)$	=	glider drag force tangent to glide path, N
e	=	Oswald's efficiency [1]
g	=	gravitational acceleration constant, m/s^2
$h(t)$	=	glider vertical position in the global 2-D space
$L(t)$	=	glider lift force normal to glide path, N
m	=	glider mass, kg
AR	=	wing aspect ratio
$R(t)$	=	radius of curvature, m
S	=	wing planform area, m^2
t	=	time, s
$u(t)$	=	glider velocity, tangent to the glide path, m/s
$x(t)$	=	glider horizontal position in the global 2-D space
$\gamma(t)$	=	glide path angle, rad
ω	=	angular velocity, rad/s
ρ	=	air density, kg/m^3

I. Introduction

IN NATURE, membrane-winged mammals exploit both gliding (flying squirrels [2–6], marsupial gliders, and flying lemurs or colugos) and flapping flight (bats). It is likely that flapping flight in bats evolved from gliding in tree-dwelling ancestors [7–13]. The glide trajectories of these extant membrane-winged mammals are characterized by short glide ranges and rapidly varying height, velocity, and glide angle. We present a dynamics model for glide range optimization in unsteady, short-range glides and apply it to biologically inspired gliders.

Energetically optimal gliding or gliding efficiency can be defined using at least two different metrics. Maximizing the horizontal travel, or glide range, for a given initial system energy (velocity and height) is the most natural definition of optimal glide efficiency. Using this efficiency metric, the work invested into climbing (increasing the potential energy) and launching (initial kinetic energy) is converted into useful glide distance. This metric represents energy conversion efficiency. An alternative metric for maximizing glide efficiency would be to minimize the energy loss during the glide. In this efficiency metric, the total vehicle energy (the sum of kinetic and potential energy) is maximized for all points in the glide. A direct consequence of minimizing energy losses is minimizing drag losses. In situations involving steady gliding flight, these two statements of glide efficiency are identical [1], however, we will show that, for transient short-range and duration glides, these two definitions of efficiency are incompatible. We will also show that for biological gliders, range maximization may be more beneficial ecologically than minimizing energy losses during the glide.

In many applications, gliding flight performance may be adequately approximated using steady-state approximations of the quasi-steady or unsteady glide. This is because the short transients associated with the initial and final conditions of the glide usually have negligible impact when compared with the longer duration of the steady-state glide. During steady-state glides, the acceleration of the glider is negligible, and maximum range is achieved when the lift-to-drag ratio is maximized. This well-known steady-state condition guarantees minimum energy loss during the glide [1] because the lift force is produced with minimal drag losses. We study short-range glide trajectories for insight into the applicability of classical steady-state glide theory in animal gliding.

We present a computational model that solves the time-dependent equations of motion to describe the glide trajectory. The ordinary differential equations describing the glide are numerically integrated using a Runge–Kutta fourth-order integration scheme. For each lift coefficient time-history, our computational model computes a unique glide trajectory. As a result, we are able to examine the effect of varying the lift coefficient on the glide range. Using MATLAB's built-in optimization toolkit, we are able to determine the best lift coefficient for each launch height considered. We show that classical gliding theory does not result in optimal range for transient glides.

Presented at the Applied Aerodynamics Conference, San Antonio, TX, 22–25 June 2009; received 12 November 2010; revision received 8 March 2011; accepted for publication 24 March 2011.

*Assistant Professor, Mechanical Engineering Department.
†Graduate Student, Department of Ecology and Evolutionary Biology.
‡Professor, School of Engineering.
§Professor, Department of Ecology and Evolutionary Biology and School of Engineering.

We find the best lift coefficient for short-range gliding to be consistently larger than the lift coefficient, which maximizes the lift-to-drag-ratio.

II. Glider Model: Theory

In our model we approximate the glider as a point mass, and perform a force balance analysis using the variables defined in Fig. 1. For a glider, the relevant forces are the time-dependent lift $L(t)$ and drag $D(t)$, which can be characterized using nondimensional coefficients $C_L(t)$ and $C_D(t)$. For convenience, we use a coordinate system that is defined by the tangent and normal unit vectors of the instantaneous glide path. The instantaneous glide angle γ is defined as negative when the glider is losing altitude. The velocities u_t, u_n and accelerations a_t, a_n, defined in the glide trajectory reference frame are the tangential and normal components. The normal velocity, u_n, is identically zero.

The momentum balance in the tangential direction can be written as:

$$\frac{\mathrm{d}|u|}{\mathrm{d}t} = a_t = -\frac{\rho u^2 C_D S}{2m} - g\sin(\gamma) \tag{1}$$

where m is the animal's mass. The force balance in the normal direction yields

$$a_n = \frac{\rho u^2 C_L S}{2m} - g\cos(\gamma)$$

The normal acceleration can also be expressed as a function of the instantaneous angular velocity $\omega(t)$ and the radius of curvature $R(t)$:

$$a_n = \omega(t) \times \omega(t) \times R(t)$$

and by rearranging the expression for the normal acceleration:

$$\omega(t) = \frac{a_n}{u} = \frac{\mathrm{d}\gamma}{\mathrm{d}t}$$

We find an ordinary differential equation to describe the change in glide angle:

$$\frac{\mathrm{d}\gamma}{\mathrm{d}t} = \left(\frac{\rho u^2 C_L S}{2m} - g\cos(\gamma)\right)\frac{1}{u} \tag{2}$$

which, when coupled to the definitions of the horizontal and vertical velocities:

$$\frac{\mathrm{d}x}{\mathrm{d}t} = u\cos(\gamma) \tag{3}$$

and

$$\frac{\mathrm{d}h}{\mathrm{d}t} = u\sin(\gamma) \tag{4}$$

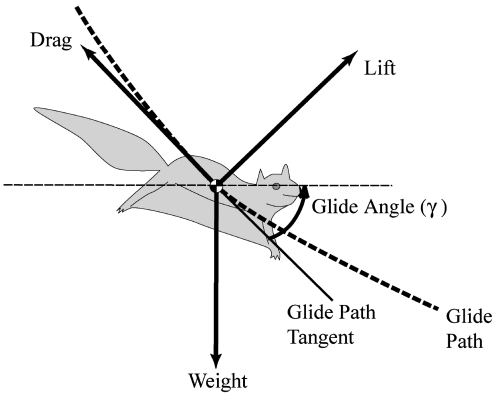

Fig. 1 A free body diagram of the glider illustrating the forces that influence glider performance; γ as shown is negative.

results in a system of ordinary differential equations [Eqs. (1–4)] that describe the dynamics of gliding flight [14]. For a given glider, the mass and the wing reference area are specified; however, the lift and drag coefficients are ultimately controlled by the glider through limb position and the shape of the wing.

Finally, we define the time-dependent energy available for the glide as the sum of the kinetic and potential energy:

$$E = E_k + E_p = \frac{1}{2}mu^2 + mgh \tag{5}$$

In most longer-range glides, the transients associated with launch and landing occur over a time period that is much shorter than the time spent in steady glide, and a steady-state analysis is an adequate approximation of the entire glide. Steady-state gliding occurs when the forces acting on the glider are in equilibrium and, as a result, there is no net acceleration of the glider. The steady-state portion of these long-range glides can be described using simplifications of Eqs. (1–4):

$$\frac{\mathrm{d}|u|}{\mathrm{d}t} = \frac{\mathrm{d}\gamma}{\mathrm{d}t} = 0 \qquad \frac{\mathrm{d}x}{\mathrm{d}t} = u\cos(\gamma) \qquad \frac{\mathrm{d}h}{\mathrm{d}t} = u\sin(\gamma)$$

The result of combining the steady-state equations is the classical steady-state glide optimization statement:

$$\frac{C_L}{C_D} = -\cot(\gamma) \tag{6}$$

To maximize the steady-state glide range, the glide path angle γ should be minimized. This is equivalent to maximizing the lift-to-drag ratio, C_L/C_D. By examining Eq. (5), we can observe that, at any two successive locations in a steady-state glide, the kinetic energy will remain the same. This implies that any potential energy reduction is a direct result of overcoming the aerodynamic drag. Hence, for a given lift, optimal steady-state energetics implies drag should be minimized.

III. Glider Model: Numerical Implementation

A. Discretization of the ODEs

For short-range glides, the transients associated with the glider's launch dominate the glide trajectory. As such, we must integrate the full time-dependent system of ordinary differential equations (ODEs) [Eqs. (1–4)]. We perform the numerical integration using a fourth-order Runge–Kutta method (MATLAB's ODE45 function).

B. Defining the Lift and Drag Coefficients

To complete the numerical implementation of the glider model, we must prescribe a lift and drag coefficient for all times during the glide. In our implementation, the time-dependent lift coefficient ($C_L(t)$) is represented using a piecewise linear discretization (Fig. 2). In our model, lift coefficient values are prescribed at specific times during the glide. Intermediate values for the lift coefficient are interpolated

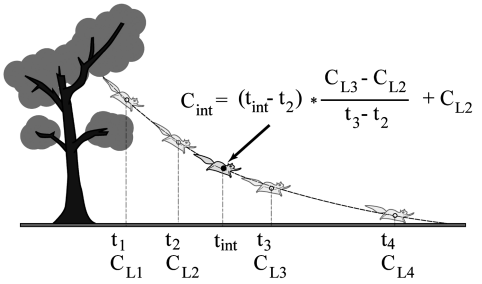

Fig. 2 The two-dimensional glide path between a launching and landing site can be characterized by a collection of lift coefficient C_L values at discrete times t during the glide. The lift coefficient C_L at intermediate points can be linearly interpolated using the discrete prescribed values.

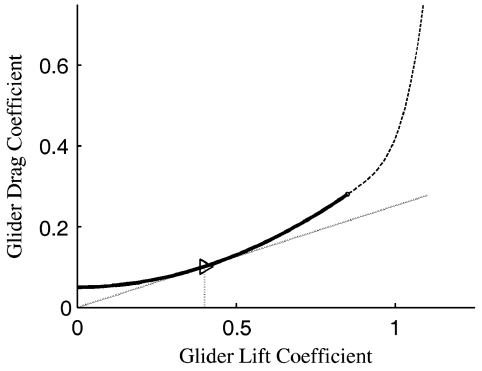

Fig. 3 The semi-empirical drag polar for the exemplar glider. The solid line ($C_L = [0, 0.85]$) represents the prestall behavior, while the dashed line ($C_L = (0.85, 1.1)$) represents the poststall behavior. Stall starts at $C_L = 0.85$. The lift coefficient at the maximum lift-to-drag ratio ($C_L/C_D = 3.8$) is also shown using a triangle symbol ($C_L = 0.4$). The maximum lift-to-drag ratio is determined by finding the line that is tangent to the drag polar and passes through the origin.

linearly using neighboring values. The drag coefficient is a function of the lift coefficient and several empirical parameters (Fig. 3):

$$C_D = C_{D_o} + \frac{C_L^2}{\pi e \mathrm{AR}} + \mathrm{bool}(C_L > C_{L_{\mathrm{stall}}}) \cdot 100 \cdot (C_L - C_{L_{\mathrm{stall}}})^4 \quad (7)$$

where C_{D_o} represents the baseline viscous component of the drag, AR is the wing aspect ratio, and e is the Oswald's efficiency parameter [1]. The second term in the equation represents the induced drag, and the last term is a stall penalty term, which rapidly increases drag when the lift coefficient exceeds its value at stall. The parameters C_{D_o}, AR, e, and $C_{L_{\mathrm{stall}}}$ are parameters estimated from measurements or aerodynamic models. The drag polar is a simple model of the actual physics of the problem, but it does serve to test the fundamental hypotheses posed in this paper.

C. Optimizing the Glide Trajectory

To determine the maximum glide range for a given initial launch height, we use MATLAB's unconstrained gradient based optimization techniques (MATLAB *fminunc* function, Mathworks, Natick, MA). The lift coefficient optimization is accomplished using the *fminunc* function to find the lift coefficient distribution that maximizes the glide range.

IV. Exemplar Glider Model and Test Cases

In this paper we model a southern flying squirrel, *Glaucomys volans* (Table 1). The predictions are based on a drag polar (Fig. 3) that is based on quasi-steady aerodynamics measurements made on a membrane wing [15]. This drag polar does not include unsteady effects such as dynamic stall or added mass, both of which may play a role in maneuvering and landing. For this polar, the lift-to-drag ratio is maximized when $C_{L_{\max(L/D)}} = 0.4$ ($\max(C_L/C_D) \simeq 3.8$).

We examine several different gliding strategies:

1) *Glide at the Maximum Lift-to-Drag Ratio ($C_L = C_{L_{\max(L/D)}}$)*: We prescribe the constant lift coefficient, which corresponds to the maximum lift-to-drag ratio. For our exemplar glider, the maximum lift-to-drag ratio is 3.8, which corresponds to a lift coefficient of 0.4. This strategy corresponds to applying the results from steady-state glide to the short-range glide problem.

2) *Glide at a Prescribed Constant Lift Coefficient, ($C_L = \mathrm{const.}$)*: We prescribe a series of different constant lift coefficients and examine glide performance.

3) *Glide at a Constant Lift Coefficient, Optimized for Maximum Range, ($C_L = C_{L_{\max(\mathrm{Range})}} = \mathrm{const}$)*: We maximize the glide range by numerically optimizing a constant-valued lift coefficient. These simulations illustrate the dependence of glide range on optimal lift coefficient and initial height.

4) *Glide at a Time-Varying Lift Coefficient, ($C_L = C_{L_{\max(\mathrm{Range})}} = f(t)$)*: We maximize the glide range using gradient based techniques by optimizing the time-varying lift coefficient.

Table 1 Computational model inputs for the exemplar glider

Input variable	Characteristic Vvalue
Initial x-Velocity	3 m/s ($\simeq 3.07 \pm 0.11$ m/s Schieibe et al. [3])
Oswald's efficiency	0.9 (est. Anderson [1])
C_{D_0}	0.05 (est. Song et al. [15])
$C_{L_{\mathrm{stall}}}$	0.85 (est. Song et al. [15])
Body mass	0.08 kg ($\simeq$ 0.081 kg Bishop [5])
Wing Span	0.150 m (est. Bishop [5])
Wing Chord	0.135 m (est. Bishop [5])

V. Results

For the exemplar glider, we define three categories of gliding: short-range (elevation losses between 0 and $23m$, Fig. 4, top-left), medium-range (elevation losses between 23 and $\sim 50m$, Fig. 4, top-center), and long-range gliding (elevation losses greater than $\sim 50m$, Fig. 4, top-right). Short-range glides are characterized by smaller elevation changes, in which the glider's velocity and glide angle vary significantly through the duration of the glide (Fig. 4, top-left and Figs. 5a–5f). The horizontal distance is highly sensitive to constant-valued lift coefficients (Fig. 4, bottom); here, lift coefficients larger than that which maximizes the lift-to-drag-ratio result in much greater glide distance. In contrast, medium-range glides are characterized by initial glide transients, followed by quasi-steady-state behavior. Medium-range glides are less sensitive to the lift coefficient across a broad range of values (Fig. 4, bottom). For the exemplar glider, the transition between short-range and medium-range glide behaviors occurs abruptly at an elevation loss of ~ 23–$24m$. At this height, the x distance travelled (~ 55–$63m$), is nearly independent of lift coefficient chosen ($0.5 < C_L < 0.85$). Long-range glides are characterized by trajectories in which the initial transient behavior associated with launch is negligible. For these glides, traditional steady-state aerodynamics gliding analysis applies, and greatest range is achieved by employing the largest lift-to-drag ratio. When lift coefficients other than the steady-state optimum are employed, the glider's range decreases.

The glide trajectories for optimized constant-lift-coefficient gliding strategies are similar overall (Figs. 5a–5f). In the first 2–$3m$ of horizontal travel, the glider experiences a rapid increase in velocity and steepening of the glide path. This quasi-freefall behavior at the beginning of the glide is dominated by gravitational acceleration because the glider velocity is too low to generate any significant aerodynamic forces. After 2–$3m$ of horizontal travel, aerodynamic forces exceed gravitational forces, indicated by an inflection point in the glide trajectory and a global minimum in the glide angle. The remainder of the glide is characterized by shallower glide angles. In the case of our exemplar glider, the glide angle remains negative throughout the duration of the glide.

For the launch heights that are examined in detail (4 to $14m$), we find that glides that employ a constant, but optimized lift coefficient are longer (larger x distance) than those in which the C_L maximizes the lift-to-drag ratio (Figs. 5a–5f). This horizontal distance increase depends strongly on the launch height; the distance traveled is 24% greater than that predicted for the maximum lift-to-drag ratio at a $4m$ launch height (Fig. 5a) to nearly triple the distance at $14m$ (Fig. 5f, Table 2). For those glides with optimized constant-valued lift coefficient, the absolute value of the glide angle is also lower than for the glider that maximizes lift-to-drag ratio (Figs. 5a–5f). The glide velocity increases rapidly for glides in which L/D is maximized, and only begins to level off toward a constant velocity for 12 and $14m$ glides. In contrast, glides with an optimized lift coefficient increase velocity more slowly. For glides from heights greater than $8m$, and optimized constant C_L, velocity does not continue to increase for the entire glide duration (Fig. 5). Again, this effect is more pronounced in glides from greater launch heights.

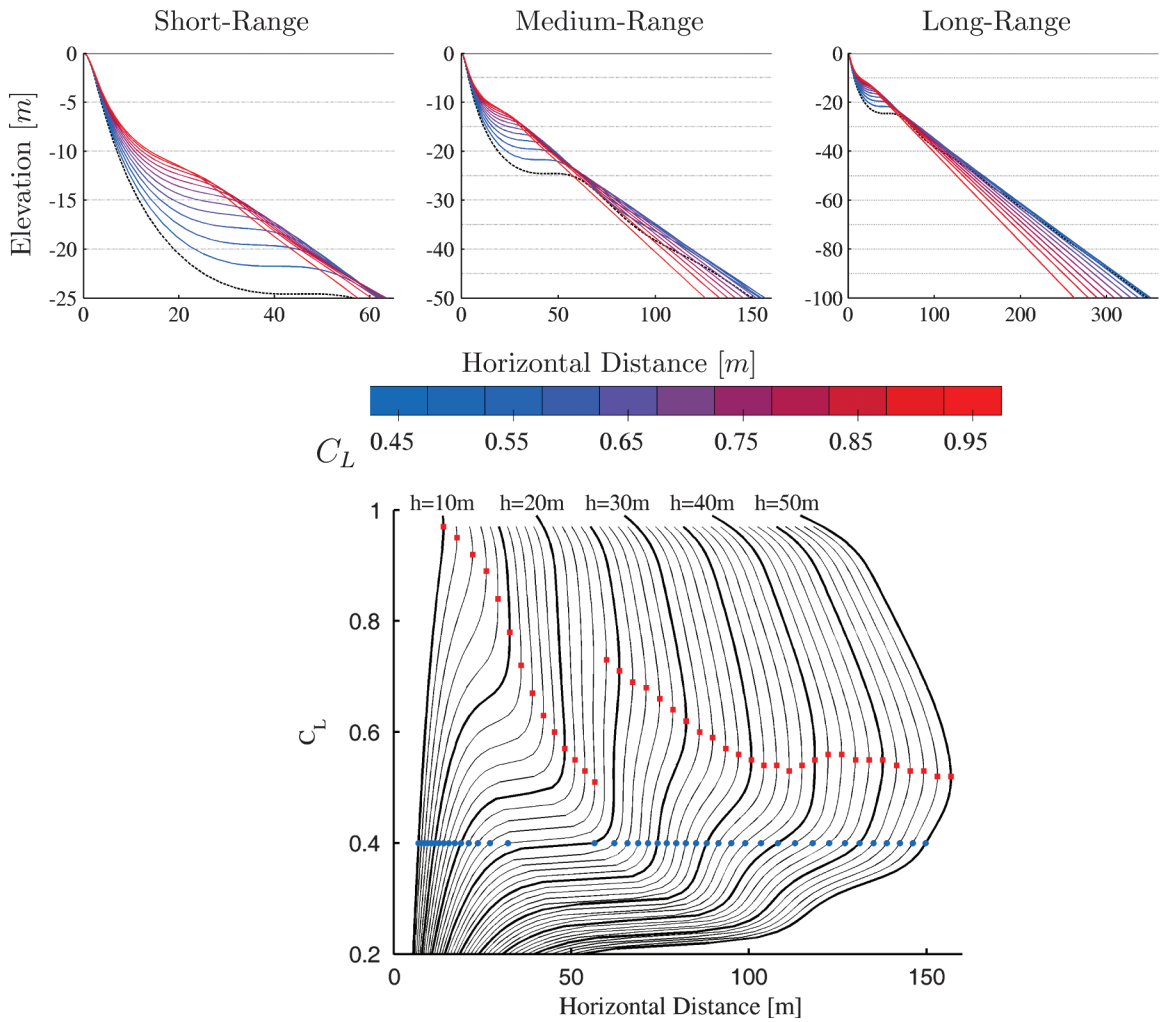

Fig. 4 Top: elevation as a function of horizontal distance for prescribed C_L between 0.4 and 0.95 in increments of 0.05. The results for the maximum lift-to-drag ratio, $C_L = 0.4$, are shown in dashed, black lines. Bottom: relationship between C_L and horizontal distance for different launch heights between 10 and 50m. The largest horizontal distance for each launch height is shown with a red marker. The horizontal distance corresponding to maximum lift-to-drag ratio is shown with a blue marker.

When the launch height is greater than 8m, we observe that the maximum glide range depends almost linearly on the launch height (Fig. 6a). For launch heights between 8 and 24m, gliders with lift coefficients that maximize range also travel significantly further than gliders that maximize their lift-to-drag ratio (Fig. 6b). For glides with an initial launch height less than 15m, maximum range occurs when glide occurs at the stall lift coefficient (Fig. 6c). When the launch height is between 23 and 24m, we observe a rapid change in the maximum range lift coefficient value (Fig. 6c). This corresponds to the transition between short- and medium-range gliding strategies. For all short- and medium-range glides, the optimal-range lift coefficient is greater than the lift coefficient that maximizes the lift-to-drag ratio.

Varying the lift coefficient as a function of time does not confer a significant performance advantage over retaining a single optimized constant lift coefficient (Table 2 and Figs. 7a–7d). This suggests that there is only a weak sensitivity of glide range to the exact functional description of the lift coefficient.

VI. Discussion

Gliding flight in nature is a successful transportation strategy in a diversity of animals. In part because of the prevalence of gliding adaptations in mammals, gliding is often suggested as an intermediate stage in the evolution of flapping flight, particularly in bat flight [7–13]. We examine gliding flight using a computational model to provide insight into parameters of importance in gliding performance. We emphasize gliding in conditions of relevance for animal gliders, which can be somewhat different from those treated in the standard aerodynamics literature [1].

A. General Characterization of Short-Range Gliding

Short-range gliding is dominated by the imbalance between weight and aerodynamic forces. The trajectories computed by our simulations demonstrate that just after launch, the glider can not generate enough lift to slow the rapid acceleration toward the ground. Once the glider reaches a velocity where sufficient lift is generated to overcome weight, the glider begins to decelerate. This behavior is seen in the glide trajectories in Figs. 4, 5, and 7.

We classify glides as either short-, medium-, or long-range (Fig. 4). In short-range glides, transient behavior dominates glide performance, and higher lift and drag coefficients are beneficial for increasing the distance traveled. The higher force coefficients generate larger forces earlier in the glide, thereby reducing the initial downward acceleration (Fig. 4, top-left). Since these glides are short in duration, reducing the downward acceleration at the expense of increased drag is a worthwhile tradeoff because this allows the glider to travel greater distances in the air. Medium-range glides are characterized by an initial transient behavior followed by a quasi-steady-state glide. Because these glides are initiated from greater heights, the initial transient glide trajectory may have a more pronounced initial acceleration and recovery (Fig. 4, top-center). Medium- and long-range glides balance the impact of initial transients with quasi-steady-state glide behavior to achieve the greatest range. As such, when launch height increases, the lift

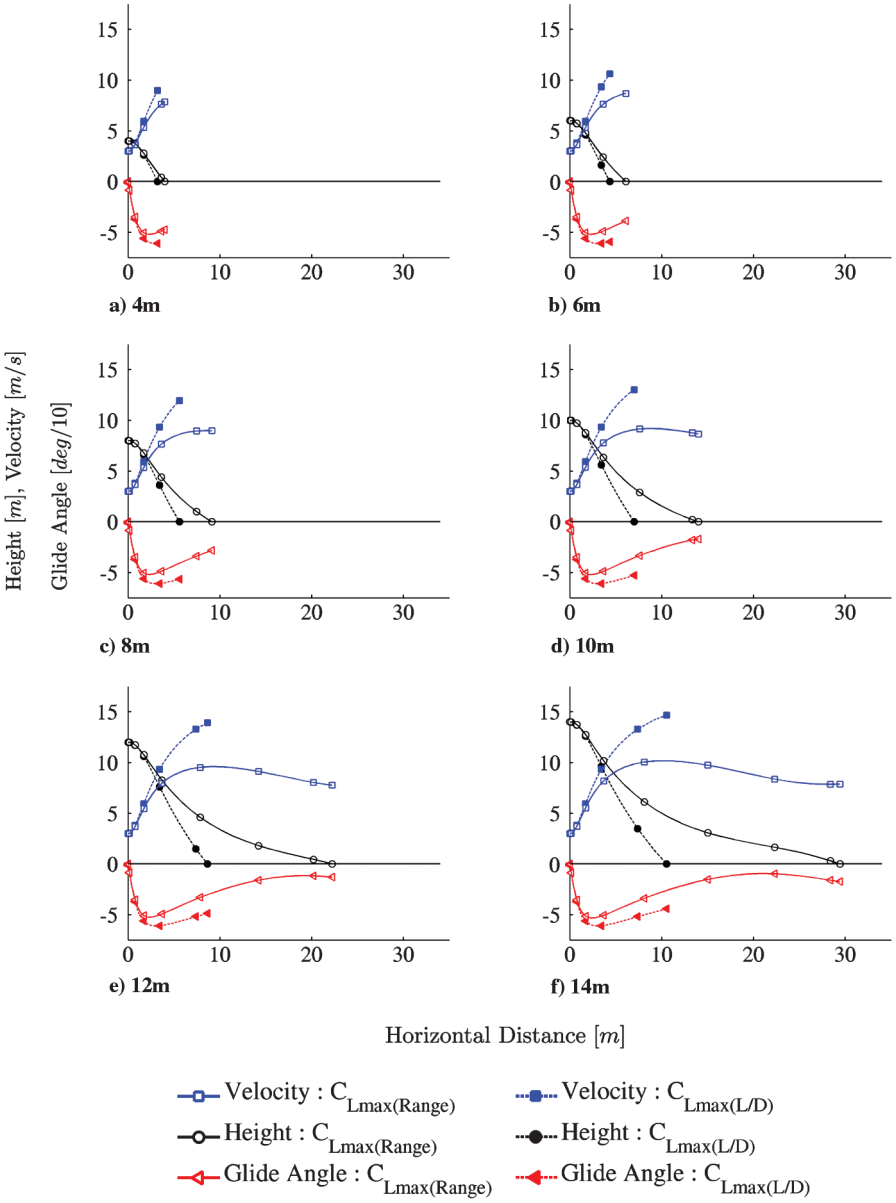

Fig. 5 Effect of launch height on glide range, velocity, and glide angle for the simulations in which lift coefficient is prescribed to maximize the lift-to-drag ratio, compared with constant-lift coefficient simulations that maximize glide range.

coefficient corresponding to maximum range asymptotes to a value that maximizes the lift-to-drag ratio.

B. C_L Variation and Optimization During the Glide

Our computational model shows that the glide range can be increased beyond the value obtained when the lift coefficient C_L is selected to maximize the lift-to-drag ratio (Figs. 5a–5f and 6a–6c). The lift coefficient value corresponding to the maximum horizontal travel has a higher value than the lift coefficient which maximizes the lift-to-drag ratio (Fig. 6c). This can be understood from both energetics and kinetics perspectives:

1. Glide Range Optimization: An Energetics Perspective

Critical to the energetics argument is the fact that any kinetic energy that must be dissipated at landing is wasted metabolic energy invested during climbing. Furthermore, excessive kinetic energy at landing may also present risk of injury to the glider. Because short-range gliders have finite time aloft, maximizing the conversion of initial potential and kinetic energy into glide range at the expense of increased drag losses is more effective than minimizing the energy lost due to drag. For example, in the glide trajectory shown in Fig. 5d, the kinetic energy at landing is more than 2 times greater for the $C_{L_{\max(L/D)}}$ simulation than it is for the case where the lift coefficient is optimized ($C_{L_{\max(\text{Range})}}$). This indicates that the glider that has conserved more energy (the $C_{L_{\max(L/D)}}$ case) will impact the landing site with a significantly greater kinetic energy than in the other case ($C_{L_{\max(\text{Range})}}$). By expending more energy during the glide, the benefits are twofold: the glider can convert energy into useful range and has less energy to dissipate upon landing.

2. Glide Range Optimization: A Kinetics Perspective

From a kinetics perspective, the unbalanced force during a transient glide contributes to increasing the linear momentum of the glider. The results indicate the maximum range lift coefficient ($C_{L_{\max(\text{Range})}}$) is consistently higher than the lift coefficient corresponding to the maximum lift-to-drag ratio ($C_{L_{\max(L/D)}}$). This also implies that the lift and drag forces in the maximum range case will typically be higher than the maximum-lift-to-drag case. As a result, the lift and drag forces can affect the net acceleration of the body differently. In Fig. 8, the forces for these two different cases are shown for an arbitrary instant during the glide, and demonstrate that the glider that operates at the maximum range lift coefficient

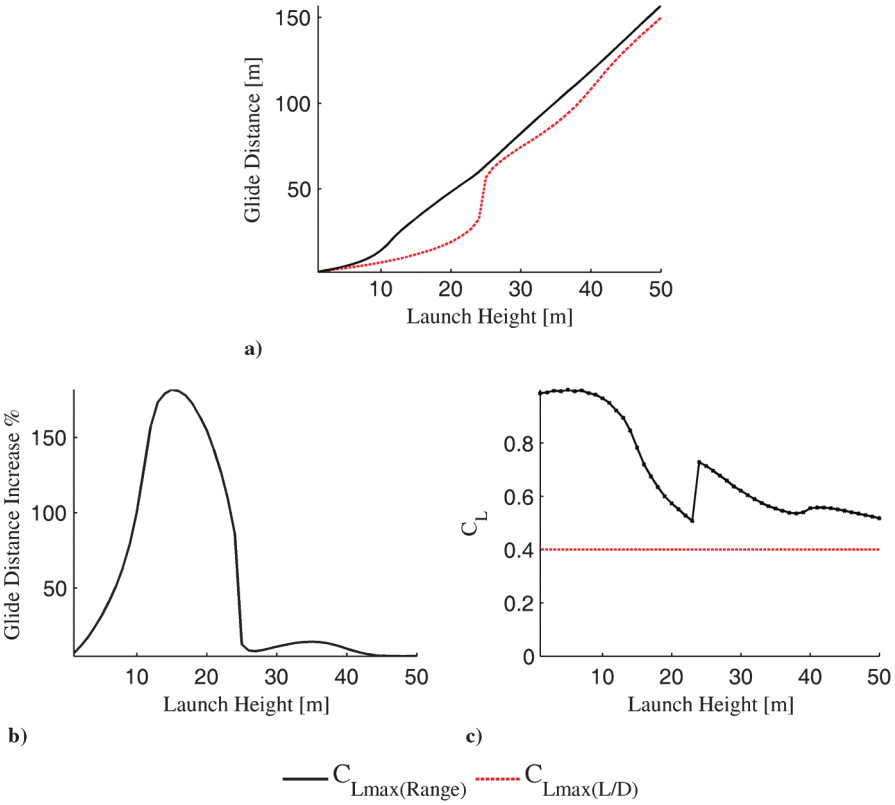

Fig. 6 a) Glide distance as a function of launch height for glides with optimized constant-lift coefficients ($C_L = C_{L_{\max(\text{Range})}}$) and with maximized lift-to-drag ratio ($C_L = C_{L_{\max(L/D)}}$), b) glide range percent improvement when a single optimal constant-lift coefficient is employed vs glides performed with a maximum lift-to-drag ratio, and c) optimal constant lift coefficient as a function of launch height; lift coefficient corresponding to maximum L/D is shown in red as a reference.

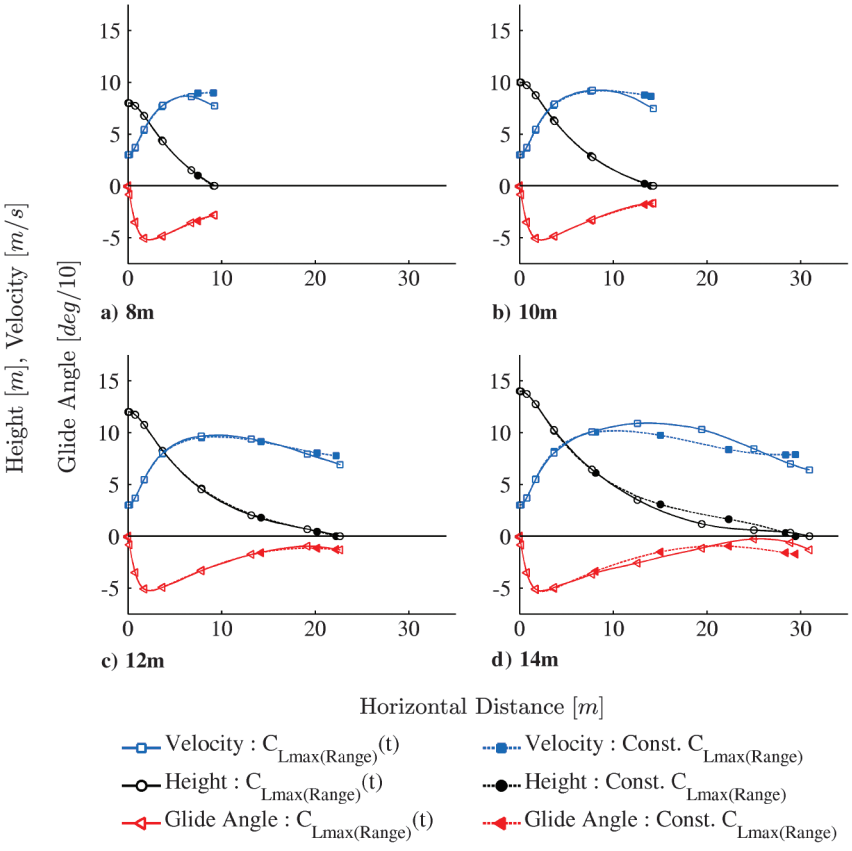

Fig. 7 Effect of launch height and lift coefficient on glide trajectory and velocity. Differences between simulations employing optimal constant-lift coefficient and time-dependent optimized lift coefficient are nearly negligible.

Table 2 Summary of simulation results; h_o = Launch height, $C_{L_1} = C_{L_{\max(C_L/C_D)}}$, $C_{L_2} = C_{L_{\max(\text{Range})}}$ = constant valued for the duration of the glide, $R_1 = R_{\max(C_L/C_D)}$, $R_2 = \max(R)_{\text{const}(C_L)}$, and $R_3 = \max(R)_{(C_L(t))}$. The range-optimal steady-state glide lift coefficient, $C_{L_{\max(L/D)}}$, is inferior to the numerically determined optimum for short-range glides ($C_{L_{\max(\text{range})}}$)

$h_o(m)$	C_{L_1}	R_1, m	C_{L_2}	R_2, m	$(R_2 - R_1)/R_1$	R_3	$(R_3 - R_1)/R_1$
4	0.4	3.21	0.99	3.99	24%	-	-
6	0.4	4.35	0.99	6.12	43%	-	-
8	0.4	5.59	0.98	9.13	63%	9.24	65.3%
10	0.4	7.00	0.97	14.00	100%	14.26	103.7%
12	0.4	8.64	0.92	22.23	157%	22.54	160.9%
14	0.4	10.54	0.85	29.42	179%	30.94	193.5%

($C_{L_{\max(\text{Range})}}$) has a resultant acceleration that slows descent. By contrast, the glider operating at a lift coefficient corresponding to the maximum lift-to-drag ratio ($C_{L_{\max(L/D)}}$) has a resultant acceleration that increases the descent rate. The kinematics diagrams indicate that despite the increased drag, the higher maximum range lift coefficient ($C_{L_{\max(\text{Range})}}$) will have a range advantage in transient glides.

C. Lift Coefficient as a Function of Launch Height

The dependence of the optimal constant-valued lift coefficient on the height of the launch is nonlinear (Fig. 6c). The range-optimal lift coefficient associated with glides with an initial elevation of 23m or less is significantly higher than the lift coefficient associated with range-optimal steady-state glide ($C_{L_{\max(\text{Range})}} > C_{L_{\max(L/D)}}$) (Fig. 6c). Although there is a different optimal lift coefficient for each glide height between ~12 and 23m, Fig. 4 (bottom) indicates that employing lift coefficients between the stall lift coefficient and the optimal lift coefficient will result in nearly optimal glide range performance. By contrast, employing a lower lift coefficient than the optimal one will result in much more rapid glide performance degradation. This indicates a performance enhancement from employing higher lift coefficients for short-range glides.

These results may explain the predominance of low aspect ratio, membrane wings among gliding mammals, lizards, and fish. Low aspect ratio membrane wings demonstrate superior performance at the higher lift coefficients desired for increased glide range. These wings possess soft stall characteristics [15], lift-reinforced camber for high lift production [15], and a beneficial pitch stability correction at high lift and in uncertain flowfields [15].¶ Biological gliders posses these beneficial characteristics of limb supported membrane wings. For initial heights of 24m and greater, the optimal lift coefficient approaches that predicted by steady-state glide analysis. This indicates that medium and long-range gliders have different aerodynamic objectives than short-range gliders.

The optimal constant-valued lift coefficient changes rapidly for launch heights between 23 and 24m (Fig. 6c). For these launch heights there is a large range of lift coefficients ($0.5 < C_L < 0.85$) that result in a similar horizontal distance (Fig. 4, bottom). This elevation marks a change in gliding strategy from short- to medium-range gliding.

D. Launch Height Dependence

Launch height is determined by the environment, and is limited by forest structure. In one natural population of Canadian northern flying squirrels [4], glide launch height was approximately 11m. In some mature forests and sloping terrain, elevation changes during gliding can exceed this value. Dudley and DeVries [16] report the heights of lowland tropical forests, postulating a correlation between glider diversity and forest canopy height. The Indo-Malayan tree heights reported by Dudley were on average 45m with individual trees having heights of 60–80m, while African and South American forests demonstrate tree heights in the range of 30–40m. Increased launch height results in substantial increases in glide range, and is accompanied by a corresponding decrease in the lift coefficient necessary to maximize glide range (Figs. 6a and 6b). Launch elevation thus plays a significant role in the choice of the lift coefficient that maximizes the glide range. This strong dependence of lift coefficient and range on launch height likely played a significant role in the evolution of specialized gliders and would likely have played a significant role in the evolution of mammalian flapping flight.

E. Sensitivity of the Glide Range to Lift Coefficient Control Resolution

When we compare glides with a constant lift coefficient to those that dynamically adjust the lift coefficient during the glide, glide range is not significantly altered by additional control of the lift coefficient during glide (Table 2 and Figs. 7). This result suggests that gliders do not benefit energetically from precise control over the lift coefficient; however, the ability to approximately prescribe optimal lift coefficients corresponding to particular launch heights is beneficial.

F. Limitations of the Glide Model

Our computational model relies on several aerodynamics and modeling simplifications. First, we constrain the analysis to two-dimensions. This assumption limits the analysis to perfectly planar glide trajectories. In reality, the glide trajectory may posses three-dimensional characteristics due to maneuvering and other lateral deviations in the flight path. These flight-path deviations will not significantly alter the total overall distance traversed by the glider; however, they will alter the point-to-point range. Second, our model uses a simplified quasi-steady aerodynamics model. Transient aerodynamics such as dynamic stall and added mass are not included in this analysis. These transient behaviors will serve to augment performance during certain parts of the glide trajectory. In particular, unsteady aerodynamics could assist gliders in extending range and reducing kinetic energy at landing by facilitating temporarily higher lift and drag coefficients. Finally, our model does not consider geometric traits such as dihedral, sweep angle, or wing flexibility, factors that have been shown to influence gliding performance in at least some animal gliders, such as butterflies [17]. Although these characteristics contribute to glide performance, our glide model focuses solely on lift and drag coefficients and not the mechanistic

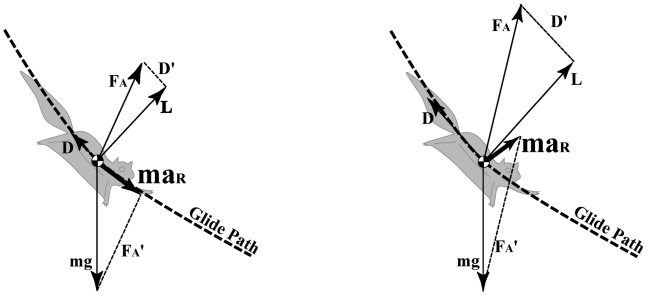

Fig. 8 Left: the force diagram for a transient glider when lift-to-drag ratio is maximized ($C_{L_{\max(L/D)}}$). Right: the force diagram for a transient glider when C_L is selected for maximum glide range ($C_{L_{\max(\text{Range})}}$).

¶Private communication with P. Ifju.

basis by which an animal produces and controls these force parameters.

VII. Conclusions

The unsteady model of gliding that was developed and presented has been used to examine glide trajectories of short-range gliders. It has been shown through numerical experiments that it is essential to consider the transient dynamics of short-range gliders when determining maximum-range or energy-optimal glide trajectories. In addition, it has been shown that the traditional steady-state optimality criterion that implies maximizing lift-to-drag ratio does not apply in the short-range gliding setting. Instead, in short-range glides, optimal distance is often achieved when lift and drag coefficients are higher than steady-state aerodynamics predicts. This strategy is successful because it slows the glider's descent and allows more time for the glider to traverse a greater distance before landing.

Acknowledgments

The authors of this paper gratefully acknowledge the support of the U.S. Air Force Office of Scientific Research-MURI on Biologically Inspired Flight for Micro Air Vehicles. The authors gratefully acknowledge the anonymous reviewers of this manuscript for their constructive comments.

References

[1] Anderson, J. D., *Fundamentals of Aerodynamics*, 4th ed., McGraw–Hill, New York, 2004.

[2] Stafford, B. J., Thorington, R. W. Jr., and Kawamichi, T., "Gliding Behavior of Japanese Giant Flying Squirrels (*Petaurista Leucogenys*)," *Journal of Mammalogy*, Vol. 83, No. 2, 2002, pp. 553–562. doi:10.1644/1545-1542(2002)083<0553:GBOJGF>2.0.CO;2

[3] Schieibe, J. S., Paskins, K. E., Ferdous, S., and Birdsill, D., "Kinematics and Functional Morphololgy of Leaping, Landing, and Branch Use in Glaucomys Sabrinus," *Journal of Mammalogy*, Vol. 88, No. 4, 2007, pp. 850–861. doi:10.1644/06-MAMM-S-331R1.1

[4] Vernes, K., "Gliding Performance of the Northern Flying Squirrel (Glaucomys sabrinus) in Mature Mixed Forest of Eastern Canada," *Journal of Mammalogy*, Vol. 82, No. 4, 2001, pp. 1026–1033. doi:10.1644/1545-1542(2001)082<1026:GPOTNF>2.0.CO;2

[5] Bishop, K. L., "The Relationship Between 3-D Kinematics and Gliding Performance in the Southern Flying Squirrel, Glaucomys volans," *Journal of Experimental Biology*, Vol. 209, No. 4, 2006, pp. 689–701. doi:10.1242/jeb.02062

[6] Essner, R. L., Jr., "Three-Dimensional Launch Kinematics in Leaping, Parachuting and Gliding Squirrels," *Journal of Experimental Biology*, Vol. 205, No. 16, 2002, pp. 2469–2477.

[7] Dudley, R., Byrnes, G., Yanoviak, S. P., Borrell, B., Brown, R. M., and McGuire, J. A., "Gliding and the Functional Origins of Flight: Biomechanical Novelty or Necessity?," *Annual Review of Ecology, Evolution and Systematics*, Vol. 38, 2007, pp. 179–201. doi:10.1146/annurev.ecolsys.37.091305.110014

[8] Norberg, U. M., *Vertebrate Flight: Mechanics, Physiology, Morphology, Ecology and Evolution*, Zoophysiology Series, Vol. 27, Springer–Verlag, New York, 1990.

[9] Norberg, U. M., "Evolution of Vertebrate Flight: An Aerodynamic Model for the Transition from Gliding to Active Flight," *American Naturalist*, Vol. 126, No. 3, 1985, pp. 303–327. doi:10.1086/284419

[10] Thewissen, J. G. M., and Babcock, S. K., "The Origin of Flight in Bats," *BioScience*, Vol. 42, No. 5, 1992, pp. 340–345. doi:10.2307/1311780

[11] Lewin, R., "How Did Vertebrates Take to the Air?," *Science*, Vol. 221, No. 4605, 1983, pp. 38–39. doi:10.1126/science.221.4605.38

[12] Savile, D. B. O., "Gliding and Flight in the Vertebrates," *American Zoologist*, Vol. 2, No. 2, 1962, pp. 161–166.

[13] Caple, G., Balda, R. P., and Willis, W. R., "The Physics of Leaping Animals and the Evolution of Preflight," *American Naturalist*, Vol. 121, No. 4, 1983, pp. 455–476. doi:10.1086/284076

[14] Shapira, I., and Ben–Asher, J. Z., "Singular Perturbation Analysis of Optimal Glide," *Journal of Guidance, Control, and Dynamics*, Vol. 27, No. 5, 2004, pp. 915–918. doi:10.2514/1.2104

[15] Song, A., Tian, X., Israeli, E., Galvao, R., Bishop, K., Swartz, S., and Breuer, K., "Aeromechanics of Membrane Wings, with Implications for Animal Flight," *AIAA Journal*, Vol. 46, No. 8, 2008, pp. 2096–2196. doi:10.2514/1.36694

[16] Dudley, R., and DeVries, P., "Tropical Rain Forest Structure and the Geographical Distribution of Gliding Vertebrates," *Biotropica*, Vol. 22, No. 4, 1990, pp. 429–431.

[17] Hu, Y., and Jinjun, W., "Experimental Investigation on Aerodynamic Performance of Gliding Butterflies," *AIAA Journal*, Vol. 48, No. 10, 2010, pp. 2454–2457. doi:10.2514/1.45156

N. Wereley
Associate Editor